

PRINTED HEATERS FOR NON-PLANAR SPACE APPLICATIONS

Dirk Godlinski⁽¹⁾, Reinhard Schlitt⁽²⁾

⁽¹⁾*Fraunhofer IFAM, Wiener Str. 12, D-28359 Bremen, Germany
Email: dirk.godlinski@ifam.fraunhofer.de*

⁽²⁾*OHB System AG, Universitätsallee 27-29, D-28359 Bremen, Germany
Email: ext.reinhard.schlitt@ohb.de*

INTRODUCTION

Thermal control of critical spacecraft equipment is very often supported by applying heater power in case it approaches the lower end of the operational temperature range. Of high interest for space application are a) heating of spacecraft propellant lines, b) heating of curved surfaces (tanks, cylinders, etc.), c) heater application on critical surfaces (CFRP structures, fibre wound spheres), and d) grounding of electrical non-conductive parts (plastics, CFRP panels).

Heaters are in most cases flexible elements consisting of an etched-foil resistive heating element laminated between layers of flexible Polyimide insulation. Proper installation is crucial to heater performance. The heater must be in intimate contact with the surface beneath, as any gaps can block heat transfer and cause a hot spot resulting in premature heater failure. Typical installation is with pressure-sensitive-adhesive. Technical constraints are possible bond failures encountered during thermal cycling in a space environment due to cohesive failure of the adhesive due to differential expansion of heater, adhesive and substrate, adhesion loss at the bond line interface due to inadequate surface preparation and blister formation in the bond line due to entrapped adhesive volatiles and air. Furthermore, heater application on curved surfaces are difficult to realize, since the baseline flat heater elements develops mechanical strain if bended. Sometimes expensive, preformed elements must be used. Heater application on irregular surfaces (structural brackets) is not possible with foil heaters. Propellant lines are generally from a Titanium alloy, which has very low thermal conductance properties. Care must therefore be taken to thermally treat the entire pipe length since heat transportation from a local heater along the pipe will not be sufficient. These constraints could lead to an increased effort in thermal analysis, verification and during thermal control hardware integration. The objective of the present paper is therefore to study and verify an alternative heater concept for spacecraft thermal control, which would avoid above-mentioned constraints.

Direct printing of coatings and structures on flat and curved surfaces with electrical conductive material can be used for electrical resistance heaters. They can be applied as homogeneous large area coating, often based on graphene-like material [1-3], or as a layout of distinct heating tracks [4-6]. In this paper the latter case is evaluated for typical space applications by means of printing technology on various space relevant substrates in order to verify space specific constraints and to provide an innovative heating system.

SAMPLE PREPARATION

Substrates and Insulation Coatings

Printed resistance heaters have been manufactured for performance analysis onto space relevant flat and curved substrates (Fig. 1). All substrates used in this project have not sufficient insulation resistant surfaces (Table 1) and need an undercoating prior to application of the heating structures. For better handling, the substrates have been cut to smaller dimensions, typically about 100 x 100 mm in size.

Two different kinds of insulation coatings have been applied. A Low Pressure Plasma Technology (CoverPLAS[®], Fraunhofer IFAM) was used to apply transparent, highly cross-linked polysiloxane-like coatings. The standard process was modified in order to obtain a hydrophilic surface finish for compatibility with the low viscous conductive inks for aerosol printing. Alternatively, a fully imidized polyimide solution in N-ethyl pyrrolidone has been used (P84, Evonik Fibres GmbH, Schörfing, Austria) and applied by a spin-coating process. Polyimide is used for coatings in the electric and electronics industry due to its electrical properties such as low dielectric constant or high dielectric strength. According to the manufacturer, these coatings withstand very low temperatures and are stable up to about 290 °C with short temperature peaks up to 400 °C. On flat substrates, spin-coating with rotational speed of 2000 to 3000 per min and subsequent curing at 80 °C for 30 min was used to apply reliable and reproducible coatings. On tubes the coating has been applied manually with a brush. On CFRP, the polyimide coating had no adhesion.

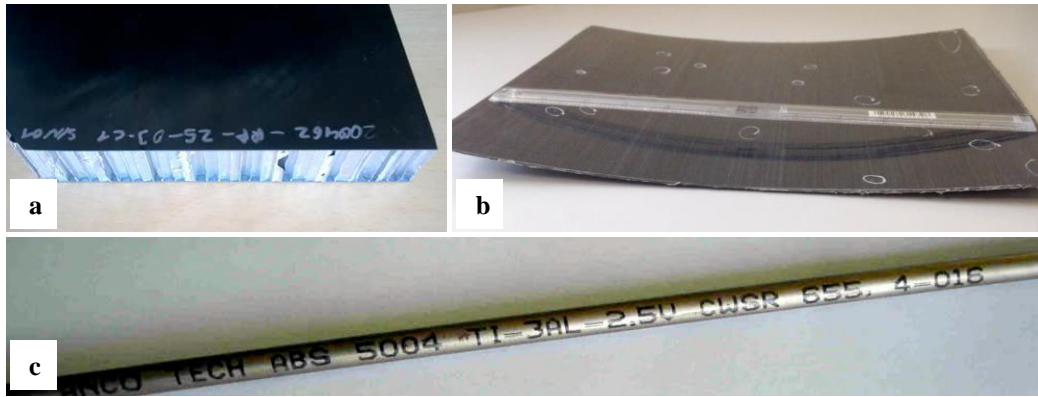


Fig. 1. Selected substrates used for application of insulating coatings and printed heaters: a) flat CFRP sandwich panel, b) curved thermoplast CF/PEEK, and c) Ti-Al-V-alloy propellant tubing.

Table 1. Typical electrical surface resistances of space relevant substrates.

Substrate material (uncoated, as received)	Specifications	Electrical Resistance (25 °C, tip distance 100 mm)
Al 6061 sheet	EN AW 6061/T6, thickness 0.65 mm	~ 1–2 Ω
Al 5754 sheet	EN AW 5754, thickness 1.5 mm	~ 0.5 Ω
Al 2024 sandwich panel	Face sheet AL 2024 T81, thickness 0.3 mm	~ 1 Ω
CFRP sandwich panel	Face sheet M55J/LTM123, 80 g/m ² , 33% RW, thickness 0.3 mm	~ 1–10 kΩ
Thermoplast curved	CF/PEEK with AS4 fibres	~ 0.2–2.0 kΩ
Ti propellant tubing	Ti 6Al-4V, 6.5 mm OD	~ 0.2 Ω

Heater Materials

Two electrical conductive materials have been used for application of heating tracks. Silver based low viscous ink with nanometer to sub-micrometer sized particles (Silverjet DGP-45LT-15C, Advanced Nano Products Co Ltd., South Korea) has been used for aerosol jetting. The ink contains spherical silver particles in triethylene glycol monoethyl ether and undisclosed additives. After drying and sintering, the solvent is evaporated and the final material consists of nearly full metal microstructure with some organic residues and pores. Second material was screen printing silver-epoxy paste for electronic applications (1901-SB, ESL Europe, UK). The paste contains silver flakes and the matrix is based on epoxy resin and butyl diglycol acetate. After drying and curing, the final material consists of a 3D network of metal in a 3D network of polymer matrix.

Printing of Heaters

After application of coatings, the heating tracks have been printed by aerosol jetting or dispensing technologies. The tracks are meanders with different distances of the parallel heating track sections and different number of slopes. The track lengths varied between 80 and 400 mm, respectively.

The Ag ink has been applied with aerosol jetting technology (M³D-103, Optomec Inc., Albuquerque, USA). This technology generates and focuses a continuous stream of aerosol droplets. The stand-off distance between nozzle and substrate is several centimetres, typically, which facilitates printing over steps and certain three-dimensional surfaces without tracking the print-head in z-direction [7]. The samples have been prepared by means of a nozzle with 150 μm diameter and printing velocities of 1–2 mm/s in 2–3 layers on top of each other. The resulting track width and height are 115 μm and 3 μm, respectively. The tracks have been cured at 150 °C for 30 min.

The Ag paste has been applied with a rotary micro-valve needle dispensing technology (Techcon Systems, California, USA) and a piezo-driven contactless micro-dispensing valve jetting technology (MDS 3000, Vermes Microdispensing GmbH, Otterfing, Germany), respectively, mounted on a special designed programmable, 3-axis CNC milling machine [4]. Needle dispensing with inner needle diameter of 100 μm and a dispensing velocity of 0.6 mm/s led to track width and height of 435 μm and 16.5 μm on plasma coating and track width and height of 555 μm and 17 μm on polyimide coating, respectively. Contactless jetting with a nozzle diameter of 150 μm and a jetting velocity of 9 mm/s led to track width and height of 1215 μm and 65 μm on plasma coating, respectively.

Application of Contacts

For testing, the printed heating tracks have been contacted with a silver plated copper wire qualified according to ESCC 3901/019 (SPL 10-26-C AWG26, W. L. Gore & Associates, Inc.). Two different bonding methods and materials have been applied. Wires have been fixed directly into the wet tracks of dispensed 1901-SB silver-epoxy paste used for the heating test structures and cured altogether. The wires were embedded with a length of about 5 and 10 mm, respectively. This method is used in-line with the dispensing of the heating structures and needs no additional manufacturing step for contacting.

The second method was used for contacting Aerosol jetted heaters by fixing the wires in a subsequent manufacturing step by means of a dispensable, silver-filled 2 K epoxy adhesive (Elecolit[®] 323, Panacol-Elosol GmbH, Germany). This adhesive for bonding open chip components has been chosen, because it shows a temperature resistance from -60 to +175 °C, has a high purity (ionic content of Na⁺, K⁺ and Cl⁻ below 10 ppm) and passed the pressure cooker test for 1000 h. The wires were embedded with a length of about 5 mm. Prepared breadboard samples with contacted printed heaters for subsequent characterisation and testing are shown in Fig. 2, 3 and 9.

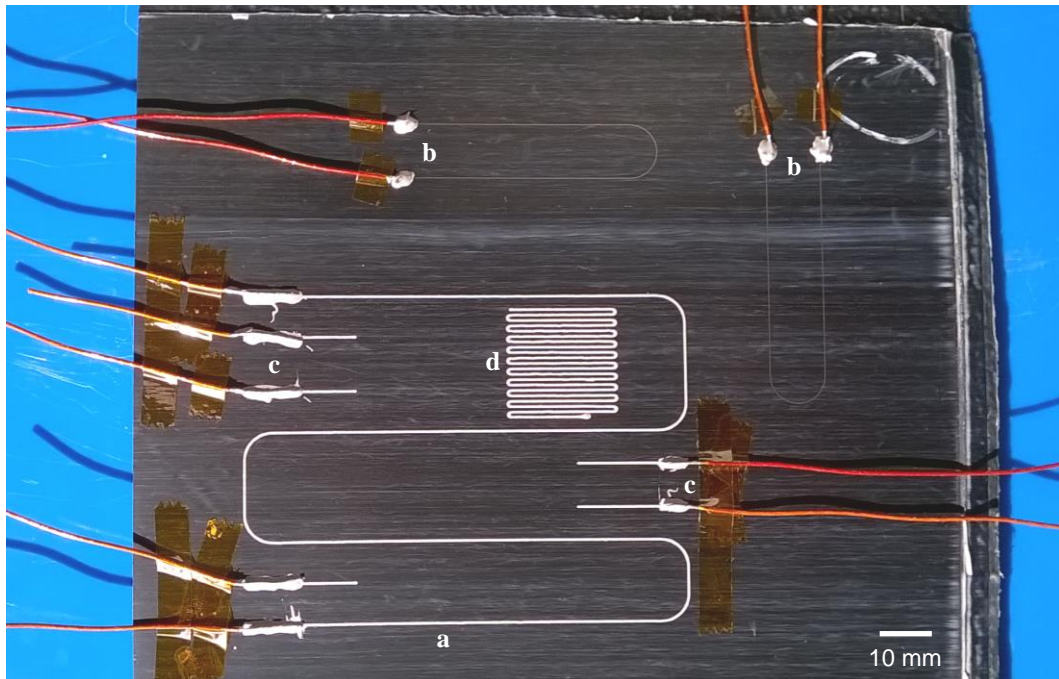


Fig. 2. Curved CF/PEEK sample with contacted **a** dispensed heater (length 400 mm), **b** aerosol jetted heaters (length 100 mm), and test structures for **c** pull-out test and **d** cross-cut test.



Fig. 3. Titanium alloy tubes with aerosol jetted and contacted heating tracks of a) 80 mm length on polyimide coating, b) 100 mm length on IFAM plasma coating.

CHARACTERISATION AND RESULTS

Electrical Insulation and Resistance

The thickness of coatings has been measured according DIN EN ISO 2360 at 5 to 10 locations distributed over the surface of each sample and mean values as well as standard deviations calculated. The electrical resistance of as received and coated surfaces has been measured with a micro-ohmmeter (Chauvin Arnoux C.A 6240, France), the

electrical isolation behaviour of coatings with an insulation resistance tester (Keysight U1461A, USA) at different locations across the surfaces.

In this study, a plasma coating thickness of $3.7 \mu\text{m} \pm 0.3 \mu\text{m}$ was applied and spin-coatings with thickness between 7.4 and $9.9 \mu\text{m}$ (Table 2). For all coatings at room temperature insulation resistances of higher than $260 \text{ G}\Omega$ (out of measuring range) at voltages up to 500 V have been measured. For plasma coatings at $85 \text{ }^\circ\text{C}$ the insulation resistance seems to decrease to typical values of higher than $66 \text{ G}\Omega$ at 100 V, especially towards the borders and edges of the samples. After application of heating tracks, the insulation resistance between tracks and coatings has been recorded. For polyimide coated samples the same results have been observed, but for plasma coated samples the insulation resistance often collapsed and shorts have been observed. Obviously with measuring tips on the coating, existing small local point defects cannot be detected on the surface but are accessible by the inks or pastes of the conductive tracks.

Depending on the heater material and the printing process the cross sections of tracks differs significantly, which is recorded in Table 3. The electrical resistivity depends on the cross section that is accessible by the electric current. A track of Ag paste having a width of 1 mm and a thickness of around 0.05 mm lead to electrical resistance around $10 \text{ }\Omega/\text{m}$ which is significantly higher compared to a pure Ag wire of 0.25 mm diameter with $0.5 \text{ }\Omega/\text{m}$, but is quite comparable to commercial Ni wires of 0.12 mm diameter or NiFe48 or NiCr20 wires of about 0.2 mm diameter. Aerosol jetted tracks can have much higher electrical resistance around $1 \text{ k}\Omega/\text{m}$ due to their small dimensions of 50 to $100 \mu\text{m}$ widths and 2 to $3 \mu\text{m}$ thickness. These printed tracks have similar electrical resistance as FeCr22Al5.8 (KAN-A1) wires of $40 \mu\text{m}$ diameter.

Table 2. Electrical insulation resistances of applied coatings.

Coating	Parameters	Thickness	Insulation Resistance IR	
			Coating/coating	coating/track
IFAM Plasma	CH_PA7_161215	$3.7 \pm 0.3 \mu\text{m}$	$> 260 \text{ G}\Omega$ (@500 V)	often shorts
P84 spin coating	2000 rpm	$9.4 \pm 0.5 \mu\text{m}$	$> 260 \text{ G}\Omega$ (@500 V)	$> 260 \text{ G}\Omega$ (@500 V)
P84 spin coating	2500 rpm	$8.7 \pm 0.4 \mu\text{m}$	$> 260 \text{ G}\Omega$ (@500 V)	$> 260 \text{ G}\Omega$ (@500 V)
P84 spin coating	3000 rpm	$7.4 \pm 0.2 \mu\text{m}$	$> 260 \text{ G}\Omega$ (@500 V)	$> 260 \text{ G}\Omega$ (@500 V)

Table 3. Spectrum of typical characteristics of printed heating tracks.

Heater Material	Printing Process	Mean Track Width	Max. Track Height	Electrical Resistance
Ag ink	Aerosoljet 2x, $v = 2 \text{ mm/s}$	$83 \pm 7 \mu\text{m}$	$2.3 \pm 0.4 \mu\text{m}$	$2800 \text{ }\Omega/\text{m}$
Ag ink	Aerosoljet 3x, $v = 1 \text{ mm/s}$	$56 \pm 6 \mu\text{m}$	$3.0 \pm 0.6 \mu\text{m}$	$1200 \text{ }\Omega/\text{m}$
Ag paste	Needle dispensing $\phi 0.1 \text{ mm}$, $v = 0.6 \text{ mm/s}$	$458 \pm 61 \mu\text{m}$	$17 \pm 1 \mu\text{m}$	$155 \text{ }\Omega/\text{m}$
Ag paste	Needle dispensing $\phi 0.1 \text{ mm}$, $v = 0.6 \text{ mm/s}$	$451 \pm 17 \mu\text{m}$	$16.5 \pm 0.5 \mu\text{m}$	$115 \text{ }\Omega/\text{m}$
Ag paste	Vermes jetting $\phi 0,15 \text{ mm}$, $v = 9 \text{ mm/s}$	$1198 \pm 32 \mu\text{m}$	$65 \mu\text{m}$	$12 \text{ }\Omega/\text{m}$

Heating Performance

The heating performance of samples has been evaluated at room temperature in air. A voltage source has been used to apply direct current up to several A up to 100 V. The resulting temperatures of the heating tracks has been documented with a thermographic camera (VarioCam, Jenoptik, Germany) and summarized in Fig. 4 to 7.

The printed heaters show nearly linear behaviour according Ohm's law between room temperature and $100 \text{ }^\circ\text{C}$ (Fig. 4). Heater structures from pastes can typically withstand current up to several amperes whereas the thin heater structures from inks fuse at currents $> 1 \text{ A}$. At low voltages respective currents the temperature rise low, at higher currents the maximum temperature of the heater is raising proportional. After 1–2 min temperature equilibrium is nearly reached. With higher current, higher temperature gradients develop between the heating track and substrate (Fig. 5). Within the measurement area, T_{max} represents the highest temperature of the heating track, whereas T_{min} represents the lowest temperature of the coated substrate. Temperature gradients within the heating track can be observed due to local differences in electrical conductivity of the heating track. The reproducibility and the variance of heaters prepared with identical processing are shown in Fig. 6. The electrical resistance of the 400 mm long heating tracks varies between $18.6\text{--}19.4 \text{ }\Omega$, with a mean value of $19.08 \pm 0.36 \text{ }\Omega$, leading to maximum and mean temperatures between $70.8\text{--}81.2 \text{ }^\circ\text{C}$ and $60.5\text{--}70.4 \text{ }^\circ\text{C}$, respectively. At 50 V the electric power is about 120 W. Additionally, the thermographs indicate the achieved degree of uniformity of a specific heater over the surface showing the local temperature variations depending on the local electrical resistance of the track. Temperature differences within a heating track rise with the applied voltage.

Aerosol jetted heaters on tubes have been evaluated up to 10 V with resulting currents of 0.2-0.25 A. The heating rate and cooling down behaviour is recorded in Fig. 7. After heating time of about 1 min maximum temperatures of 80 °C are achieved. After turning the power off, the temperatures decrease within 1 min down to almost room temperature.

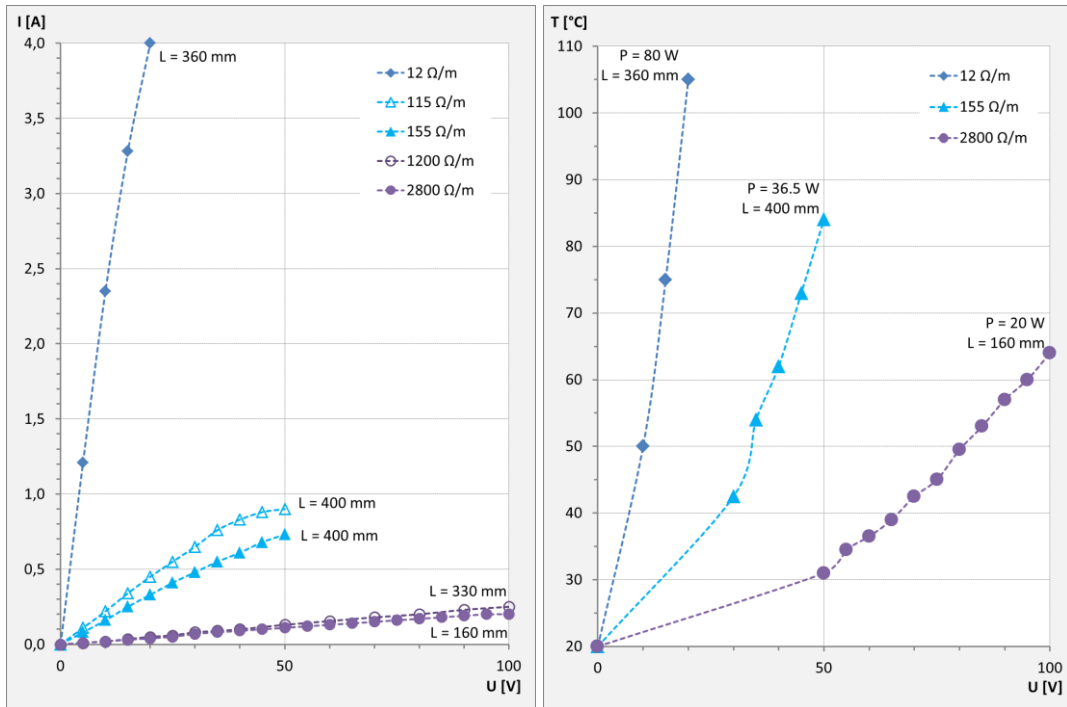


Fig. 4. Heating performance (room temperature, air) of different processed printed heaters onto coated aluminium sheets at different voltages (see Table 3 for reference). Maximum temperatures of heaters measured after 60 s.

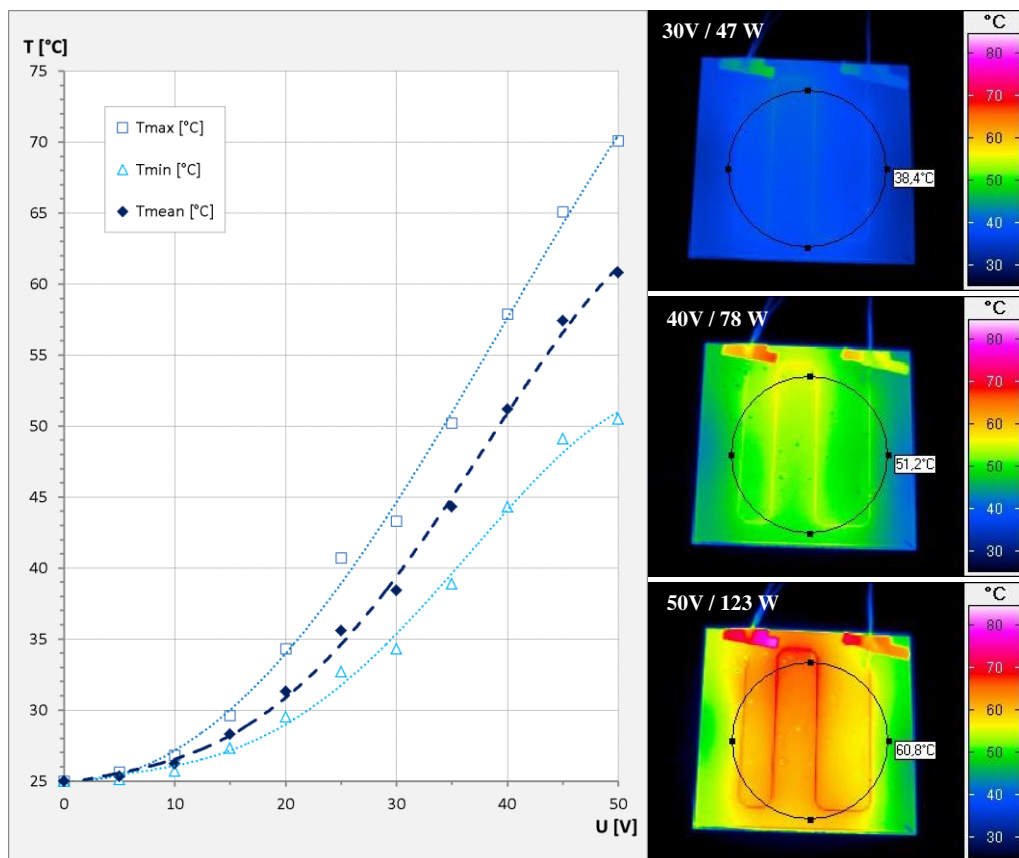


Fig. 5. Heating performance (room temperature, air) of a dispensed heater ($R = 50 \Omega/m$, $l = 400$ mm) onto polyimide coated aluminium sheet at different voltages. Resulting temperatures measured after 60 s for each voltage, T_{max} , T_{min} and T_{mean} calculated from circular area.

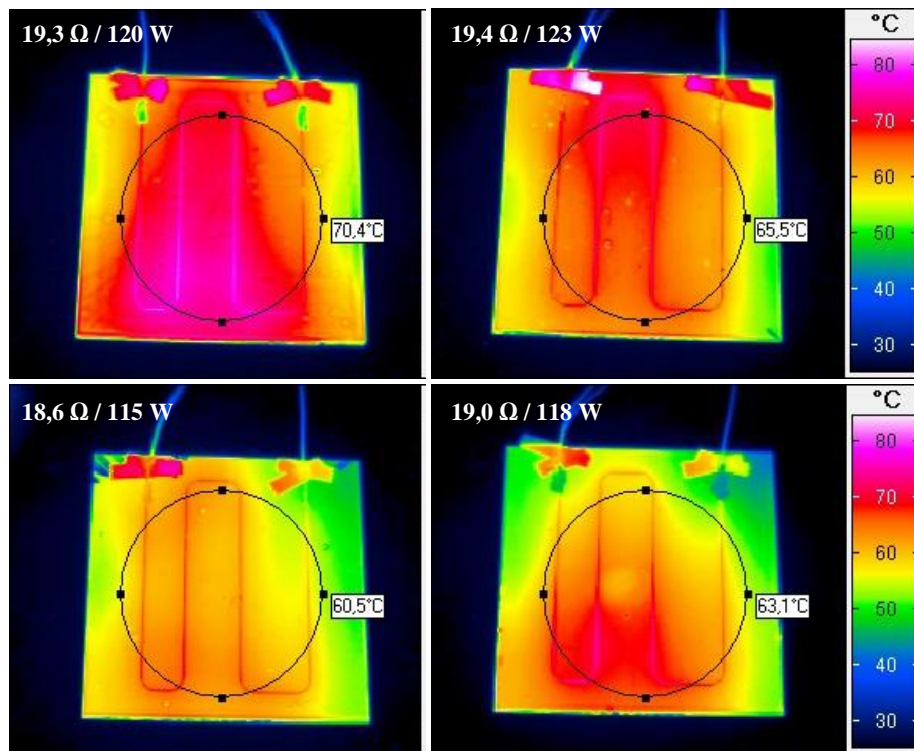


Fig. 6. Heating performance of four samples ($R = 45\text{-}50 \Omega/\text{m}$, $l = 400 \text{ mm}$) with identical processed heaters (room temperature, air) at 50 V after 90 s. Temperatures in box are mean values within circular area.

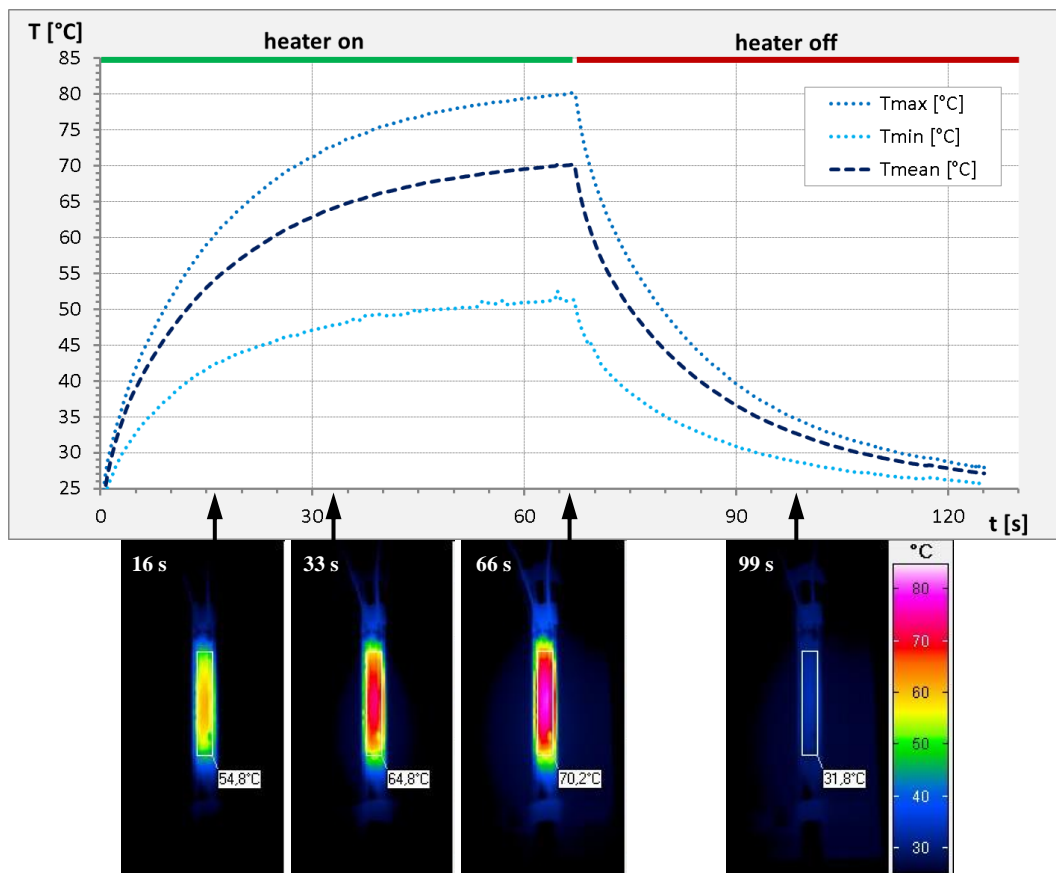


Fig. 7. Heating performance (room temperature, air) of aerosol jetted heater (see Fig. 3a, $R = 625 \Omega/\text{m}$, $l = 80 \text{ mm}$) on polyimide coated Ti tube at 10 V / 2 W. Temperatures in box are mean values within rectangular area.

Some printed heaters failed during testing (Fig. 8). This is probably caused by inhomogeneity like particle agglomerates or polymer and gas bubbles within the heating track material or by instable printing processes. Fig. 8a shows the

damage on a needle dispensed heater (track width 0.5 mm) from Ag paste after heating test. This heater showed first local defects (cracking noise and sparking) above 35 V and electrical currents higher than 0.8 A, and finally failed at 50 V completely. Typical damage on plasma coated samples is due to shorts between heating track and substrate. The plasma coating is not homogeneous especially too thin towards edges and borders (Fig. 8 b).

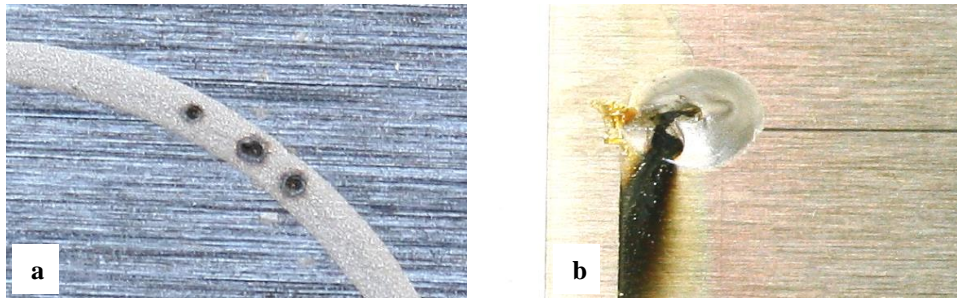


Fig. 8. Defects of printed heaters on IFAM plasma coated aluminium after electrical testing: a) needle dispensed heater failed at 50 V, and b) aerosol jetted heater contact failed at 75 V due to insufficient electrical insulation towards the aluminium substrate.

Mechanical Performance

The mechanical strength of the bonds between wires and printed heating tracks has been evaluated by a tensile testing machine (Tensor, Innwep GmbH, Würzburg, Germany) using a standard setup (MIL-STD-202 Standard Electronic and Electrical Component Parts, method 211, test condition A at 1.36 kg). Fig. 9 shows a sheet with several bonds (five already tested) during testing of the lead-pull strength and Fig. 10 the typical damage patterns.

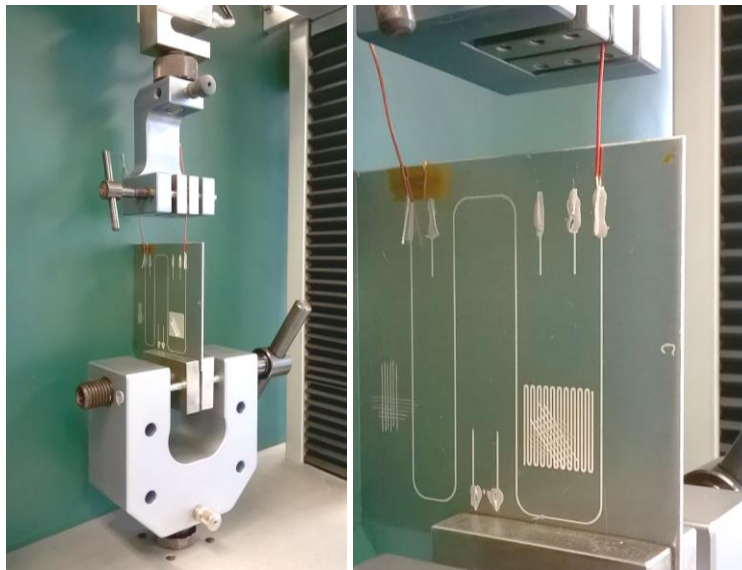


Fig. 9. Aluminium sheet with wiring in tensile testing machine for determination of lead-pull strength.

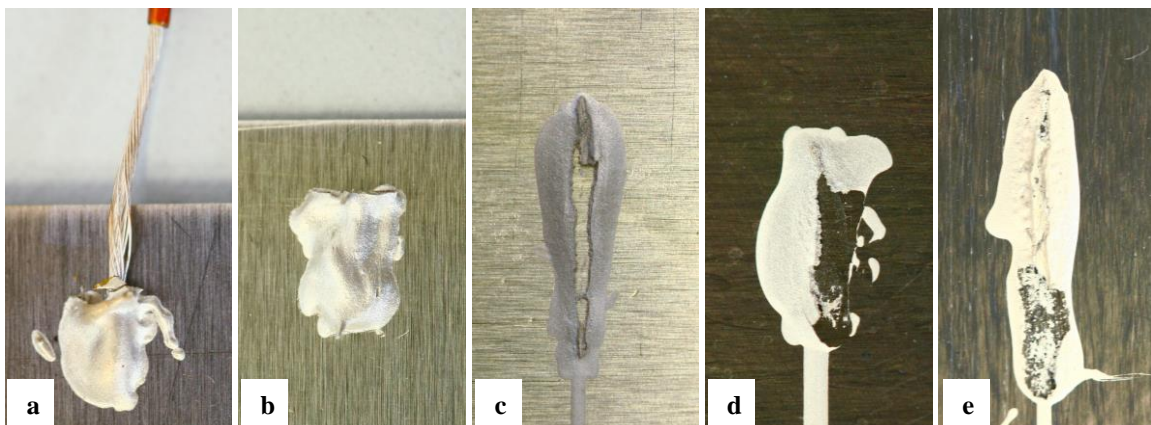


Fig. 10. Damage patterns onto different substrate surfaces after pull-out test (Elecolit 323: a and b; 1901-SB: c, d, and e). See Table 4 for reference.

Table 4. Pull-out strength of wires SPL 10-26-C AWG26 (required threshold 1.36 kg = 13.34 N).

Embedding material	Coating of substrate	Embedding wire length	No. of samples	Pull-out strength (mean value)	Damage pattern
Elecolit 323	IFAM Plasma on aluminium	5 mm	2	47.6 N	Fig. 10a
Elecolit 323	IFAM Plasma on CFRP	5 mm	2	— ¹	
Elecolit 323	P84 on aluminium	5 mm	2	38.9 N	Fig. 10b
1901-SB	IFAM Plasma on aluminium	5 mm	2	15.7 N	
1901-SB	IFAM Plasma on aluminium	10 mm	3	29.3 N	
1901-SB	P84 on aluminium	5 mm	2	13.0 N	
1901-SB	P84 on aluminium	10 mm	4	29.4 N	Fig. 10c
1901-SB	IFAM Plasma on CFRP	5 mm	2	19.6 N	
1901-SB	IFAM Plasma on CFRP	10 mm	3	23.8 N	Fig. 10d
1901-SB	IFAM Plasma on CF/PEEK	5 mm	1	5.3 N	
1901-SB	IFAM Plasma on CF/PEEK	10 mm	4	25.7 N	Fig. 10e

¹ wires including adhesive detached from substrate during handling

The lead-pull strength is in most cases sufficient as can be seen from Table 4. The adhesive Elecolit 323 develops very strong bonds onto plasma and polyimide coatings, respectively, that the wires could not be pulled out of the adhesive (see Fig. 10 a and b). Only on plasma coated CFRP was the adhesion so bad that the bonds detached already during handling (probably due to insufficient plasma coating towards the edges of the sample where the contacts are located). The Ag paste 1901-SB that has been used for heating tracks adheres sufficient towards the substrates and towards the wire. The wires are pulled out of the bonds in all cases and from the resulting patterns can be seen that the adhesion of the paste towards the wire seem to be slightly stronger than towards the substrate (Fig. 10 c-e). Using the Ag paste, embedding the wire of about 5 mm is in some cases not sufficient (pull-out strength < 13.34 N) but for about 10 mm the pull-out strength is between 23.8 and 29.4 N.

Adherence behaviour of the isolation coatings towards the substrates and of the printed heater structures on the coatings has been evaluated according to ISO-2409: 2007 "Paints and varnishes - Cross-cut test". For this test, parallel notches of 1 mm distance through the coatings and printed structures are made by means of a scalpel (Fig. 11 and 12a). Additionally, adhesive tape is applied and teared off; the resulting pattern is optically observed (Fig. 12b). The adhesion of coatings and Ag paste is good towards plasma and polyimide coated aluminium, respectively, but bad for plasma coated CFRP (Fig. 11c). Aerosol jetted Ag ink adheres less on plasma coatings compared to Ag paste (Fig. 12).

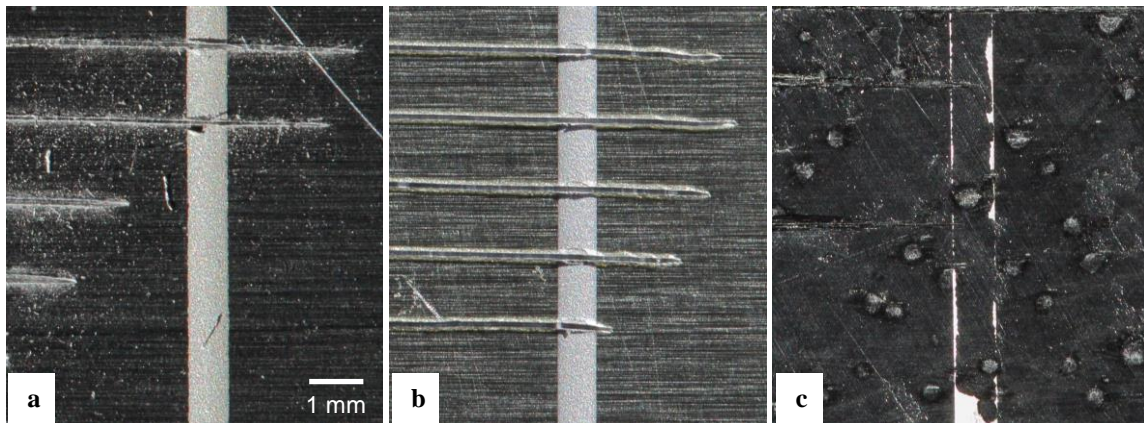


Fig. 11. Dispersed heating tracks after cutting and tape testing on a) plasma coated aluminium, b) polyimide coated aluminium, and c) plasma coated CFRP.

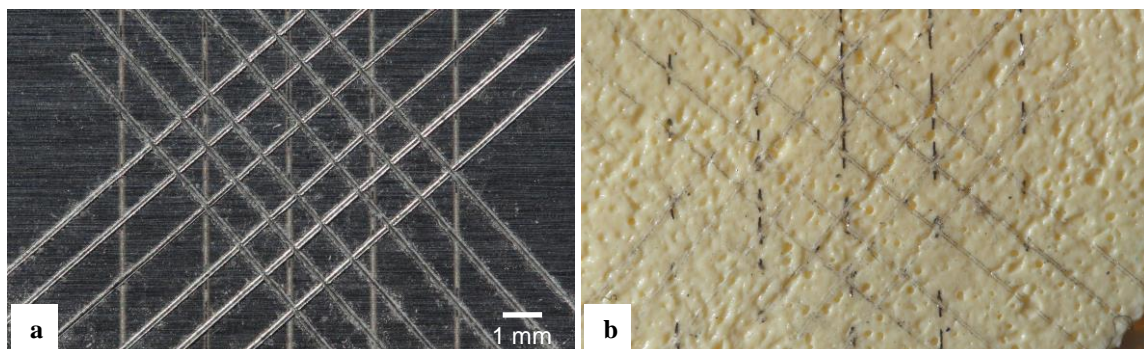


Fig. 12. Aerosol jetted heating tracks (vertical lines) after cross-cut test a) on plasma coated aluminium, b) material adherence on tape.

DISCUSSION

Coatings

Typical surfaces of space relevant parts consisting of metal or CFRP need to be coated with an electrical insulation for direct printing of heaters or sensors. Highly cross-linked polysiloxane-like plasma coatings are possible over large and 3D surface areas. They adhere well on space relevant substrates and are only few μm thin but the electrical insulation properties are found to be inhomogeneous and insufficient especially towards edges and borders. As expected, the electrical insulation properties of polyimide coatings are very good and reproducible up to 500 V. These coatings prepared by fully imidized polyimide solution can be applied on large area by various technologies like spin-coating, dip-coating, and spraying or locally by jetting with a thickness of several μm . They adhere well on space relevant metal substrates but are not suited for directly coating of carbon fibre based composites.

A top coating of the printed heaters has not been evaluated so far but could be necessary for space applications as protection against mechanical damage during handling and integration on ground. Furthermore, a top coating could be beneficial for better heater adhesion and abrasion resistance especially for very thin aerosol jetted heating tracks. Both evaluated coatings for electrical insulation can be used as top coating, plasma and polyimide.

Heaters

Silver particle filled epoxy as well as nano-particulate silver inks have been used as heater material in this study, but other metals and alloys can be used in principle for this purpose. The final tracks show relating to length electrical resistances in the range from 10 to 1000 Ω/m which is comparable to commercial resistance wires, e.g. out of Ni or NiCr alloy. For heaters from paste with thick cross section and good electrical conductivity electric power of more than 100 W is achieved with currents of several amperes. In this case, depending on the layout, up to 20 W/cm^2 are possible if the parallel heating tracks have a distance of only 2 mm to each other. The heaters from ink with small cross section withstand typically currents significantly below 1 A, having electric power of 2–20 W and around 1 W/cm^2 for parallel tracks with 2 mm distance. For comparison, the current capacity of commercial foil heaters (Polyimide Thermofoil™ Heaters, Minco Products, Inc.) is in the range of 3–13.5 A. At room temperature and in air maximum temperatures above 100 °C can be easily achieved after heating of about 1–2 min.

Aerosol jetting and dispensing are typical one-nozzle technologies and therefore relatively slow printing processes but can be scaled-up by parallel use of nozzles or print heads. Furthermore these processes can be prone to variation. Commercial foil heaters have a resistance tolerance of $\pm 10\%$ or $\pm 0.5\ \Omega$. Printed heater with silver paste are typically within this values (see Fig. 6), but aerosol jetted heaters can have higher variations. In-line control in industrial processing equipment would be helpful to achieve higher degree of reproducibility in respect of the production of identical heaters with more homogeneous heating tracks. Screen or stencil printing is a fast and higher reproducible alternative in case of flat surfaces. Besides furnace treatment of coatings and heating structures for production the treatment with IR lamps or Xe flashes could be beneficial in terms of speed and especially for large parts and components already equipped with thermal sensitive elements.

The commercial foil heaters have a total thickness of about 0.4 mm including 0.1 mm foil backing which leads to unwanted high thermal gradients between heating structure and basic substrate. The applied polyimide coatings in this study are less than 0.01 mm thick, therefore the build-up of a significant minor thermal gradient is expected, but has to be verified.

The configuration of the printed heaters with space qualified wires is possible by subsequent bonding with electrically conductive adhesive or in-line with identical heater paste material. The strength of the bond is sufficient with typical values $> 20\ \text{N}$ on almost all evaluated space relevant substrates.

Perspective

The design of the heater structure depends on the desired maximum temperatures and the applied voltage. A single meander can be used with a suitable length of the heating track. Alternatively, several parallel heating tracks can be combined in a bus-bar design. Using the printing approach, the heaters can be individually designed and tailored for a specific need and part geometry almost without processing restrictions.

Outgassing tests and ageing behaviour of the used materials, heating tests of printed heaters under vacuum or operating tests under thermal cycling will be important steps to characterise the quality and long term stability and to better understand the suitability of printed heaters on the way of qualification for space applications.

CONCLUSION

The concept of printing heaters on structural spacecraft surfaces may replace the commonly used heater foil solution by avoiding some of their inherent limitations. In addition the printed conductive structures may be applied on non-conductive substrates, which improve the ability for equipment grounding, replacing the currently used grounding rail approach. With the same printing concept it is basically possible to print temperature sensors as well on spacecraft surfaces. The benefits for space applications are free design of heater path configuration to tailor the operating temperature range to space needs, and reduced effort to integrate heaters and temperature sensors on spacecraft surfaces such as structural panels and equipment housings, on propellant lines, on curved surfaces and on irregular surfaces (valves, brackets, etc.). Precondition for introducing the printing technology during spacecraft AIT is the application of heaters off-line, i.e. the heater must be applied on parts before they are integrated into the spacecraft. This sequence supports the trend to accept fully pre-integrated sub-assemblies on spacecraft integration level.

ACKNOWLEDGEMENT

This work was partly funded by ESA under the ITI Program "Printed Heaters and Sensors". We acknowledge especially the support of Léo Farhat and Denis Lacombe from Product Assurance and Safety Department of ESTEC.

REFERENCES

- [1] G. Wróblewski, K. Kielbasinski, B. Swatowska, J. Jaglarz, K. Marszalek, T. Stapinski, and M. Jakubowska, "Carbon nanomaterials dedicated to heating systems," *Circuit World*, vol. 41, pp. 102-106, August 2015.
- [2] H. Nguyen Bich, and H. Nguyen Van, "Promising applications of graphene and graphene-based nanostructures," *Advances in Natural Sciences: Nanoscience and Nanotechnology*, vol. 7, June 2016.
- [3] Y. Yao, K.K. Fu, C. Yan, J. Dai, Y. Chen, Y. Wang, B. Zhang, E. Hitz, and L. Hu, "Three-Dimensional Printable High-Temperature and High-Rate Heaters," *ACS Nano*, vol. 10, pp. 5272-5279, May 2016.
- [4] D. Godlinski, E. Taubenrauch, C. Werner, I. Wirth, V. Zöllmer, and M. Busse, "Functional Integration on Three-Dimensional Parts by means of Direct Write Technologies," *Fraunhofer Direct Digital Manufacturing Conference DDMC2012*, Berlin, 14th-15th March 2012.
- [5] M. Kohl, G. Veltl, and M. Busse, "Printed sensors produced via thick-film technology for the use in monitoring applications," *Procedia Technology*, vol. 15, pp. 107-113, 2014.
- [6] D. Godlinski, "Flexible Sensorintegration: Schlussbericht im Verbundprojekt: Design und flexible Integration von Sensoren aus Nanodispersionen zur Strukturüberwachung - DEFIS," *Schwerpunkt Mikrosystemtechnik im BMBF-Förderprogramm: IKT 2020 - Forschung für Innovationen*, Fraunhofer-Inst. für Fertigungstechnik und Angewandte Materialforschung IFAM, Bremen, 2014.
- [7] V. Zöllmer, M. Müller, M. Renn, M. Busse, I. Wirth, D. Godlinski, and M. Kardos, "Printing with aerosols – A mask less deposition technique allows high definition printing of a variety of functional materials," *European Coatings Journal*, vol. 7-8, pp. 46-50, 2006.

AUTHORS

Dirk Godlinski studied Chemical Engineering (Dipl.-Ing.) at Clausthal University of Technology and received his PhD at University of Bremen, faculty of Production Engineering (Dr.-Ing.), in 2002.

Today, he is working at the Fraunhofer Institute for Manufacturing Technology and Advanced Materials IFAM in Bremen (Germany). As Project Manager he is involved in public funded as well as industrial R&D projects in the fields of Nanotechnology, Additive Manufacturing and Functional Printing. His current research interest is focussed on digital and additive manufacturing processes for integration of sensors and electronics into and onto 3D parts.

